

Broad immunophenotyping panel to identify and sort immune relevant cellular subsets from healthy and immunomodulated mouse lung

Luise Sternberg, Virginia Aragon

Abstract

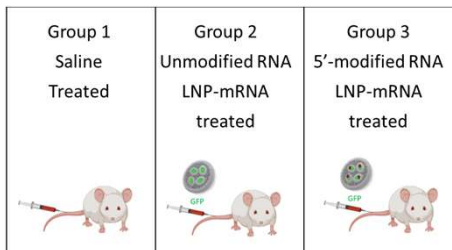
Lung inflammation, disease and dysfunction can have many causes, such as infection with viruses, and bacteria, as well as allergic reactions to environmental agents. In addition, pharmacological agents such as lipid nanoparticles can change the immunological landscape of the lung. Because of the clinical significance of the lung as a barrier organ, it is essential to understand the immune composition of pulmonary tissue. Therefore, it is key to utilize available mouse models of lung pathology. However, previously many immunophenotyping panels focused on human PBMCs and were not able to identify some of the key players in the immune response to pathogens, allergens and pharmacological agents that are found in complex tissues such as the lung. Thus, we designed and developed an immunophenotyping panel that can identify a great variety of different immune cells and other non-immune tissue resident cells subsets using spectral flow cytometry. Using this novel tool, we were able to distinguish and sort CD4+ and CD8+ T cells subsets, neutrophils, macrophages, dendritic and endothelial cells from healthy and immunomodulated lungs. While the panel is high parameter, it is still versatile enough to be used on different spectral cytometry platforms without adjustment. The combination of markers we chose can be used on its own or serve as a backbone and can be combined with other tertiary antigens to further delineate rare cell subsets or study individual antigens of interest. This novel immunophenotyping panel for murine pulmonary tissue has great potential to elucidate the details of lung pathology in many different mouse models of pulmonary dysfunction.

Introduction

Figure 1. Broad mouse lung immunophenotyping panel in a 6-laser Invitrogen™ Bigfoot™ Spectral cell sorter panel design grid
Antigen fluorochrome combinations were listed in their peak channels. Green fluorescent protein (GFP) is highlighted in green. Two open spots for additional tertiary antigens of interest are highlighted in yellow

UV 349	Marker	V 405	Marker	VB 445	Marker	B 488	Marker	Y 561	Marker	R 640	Marker
387/21	CD45 BVU95	420/10	Sca-1 BV421								
426/20		434/17									
434/17		455/14	CD31 eF450								
455/14				465/22	CD103 BV480						
473/15		473/15									
507/19		507/19	Nhp46 BV510	525/36		507/19	GFP				
549/15		549/15				549/15					
575/15	B220 BVU563	575/15	CD11b BV570	583/30		583/30		575/15	CD44 PE		
								589/15			
615/24	Ly6G BVU615	615/24	CD62L BV605			615/24	CD4 NB610-70s	605/15			
								625/15			
670/20	F4/80 BVU661	661/20	pDCA1 BV650	650 LP		670/20	Siglec F NB660-120s	661/20	CD64 PE-Cy5	670/20	CD31 APC
								685/15			
								700/13			
726/40		720/20	CD8 BV711			720/20	lgGAM PerCP-eF720	720/24		720/24	MNCHI NR720
750 LP	CD40 BVU737	747/13	CD31c BV750			750 LP		760/50	CD144 PE-Cy7		
		770 LP	Ly6E BV785					800/12		770 LP	PVD eF780
								832/37			
								860 LP			

Figure 2. Experimental model used to test the immuno-monitoring capacity of the mouse lung panel
Group 1-Control mice were saline treated to simulate handling stress (Saline). Group 2- Mice were treated with unmodified mRNA containing lipid nanoparticles (LNPs) that were predicted to cause immune changes in the mouse lung (Unmod). Group 3 - Mice were treated with the same LNP composition, but a 5'-modified mRNA was used to test whether immune changes were derived from the RNA or the LNP (Mod).



Results

Figure 3. Gating strategy overview

Flow plots of the saline treated mouse lung identify a number of non-immune lung cells such as epithelial cells and subtypes of endothelial cells. B cells, plasmacytoid dendritic cells (pDCs) and a large number of myeloid cell subtypes could be delineated within the CD3-immune cell sub compartment. Additionally, the antibody panel was able to differentiate several subtypes of tissue resident macrophages and assess their expression of activation markers. Finally, the activation and memory status of CD4 and CD8 positive T cells was investigated using key marker such as CD62L, CD44, Sca1 and Ly6C

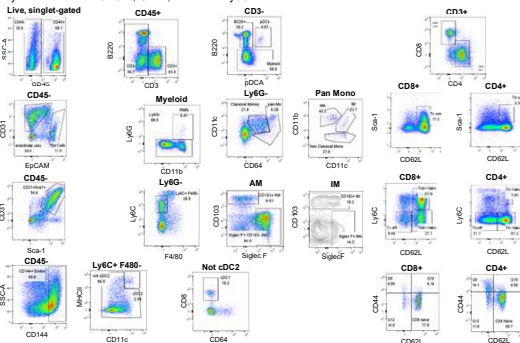
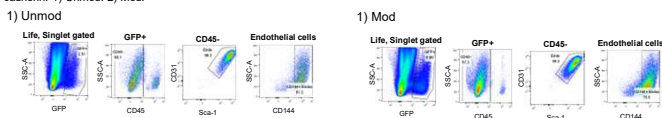


Figure 4. Tracking GFP+ lipid nanoparticles using the broad immunophenotyping panel

The LNPs could be tracked using the CD45- CD31+ Sca-1+ endothelial cell subtype. A high percentage of the LNP target cells expressed VE-cadherin. 1) Unmod. 2) Mod.



Results cont.

Figure 5. Tracking large scale immune changes

Shown are the frequency graphs (A) and flow plots (B) of the subsets most significantly affected by immunomodulation using unmodified mRNA LNP as compared to saline and Mod mice. Cell types significantly affected by immunomodulation included (1) Sca-1+, CD4+ T cells (Tc scm), (2) Sca-1+, CD8+ T cells (Tc scm), (3) Ly6C+ CD4+ T cells, (4) CD40+ B cells, (5) Ly6C+ F4/80- cells (monos), (6) B220+ pDCA+ dendritic cells (pDCs), (7) CD103+ alveolar macrophages (AMs), (8) CD103+ interstitial macrophages (IMs) and (9) Polymorphonuclear leukocytes (PMNs). Finally, profiles for endothelial cells (10) are included to illustrate that this cell subset did not change in frequency or CD144 expression

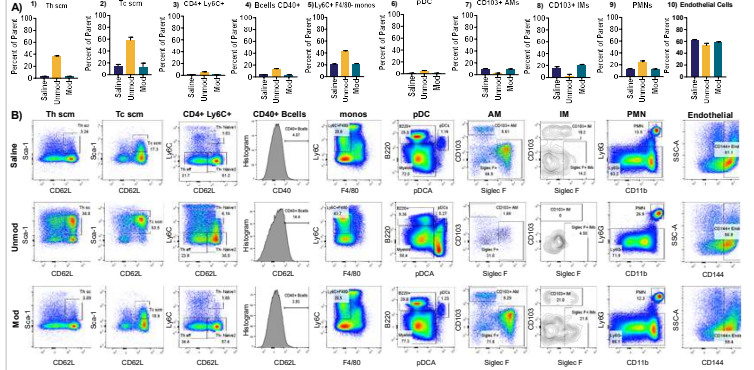


Figure 6. Consistently high sorting efficiency across different mouse treatment types and experiments

Over two experiments 9 populations from the 12 different mice were sorted using the Bigfoot Spectral Cell Sorter. The sorts were performed using a 100uM nozzle in purity mode. Some cell types were chosen because they changed drastically with immune modulation. Shown is the average sorting efficiency for each subpopulation across all sorts for (1) Tc scm (2) pDC, (3) AM, (4) PMN, (5) conventional type 1 dendritic cells (cDC1), (6) conventional type 2 dendritic cells (cDC2), (6) CD103+ dendritic cells (DC), (8) Epithelial cells (Epi) and (9) GFP+ cells

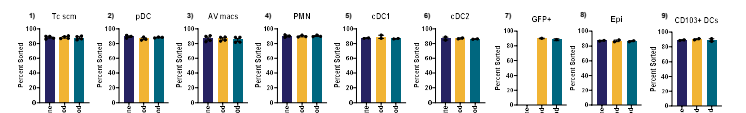
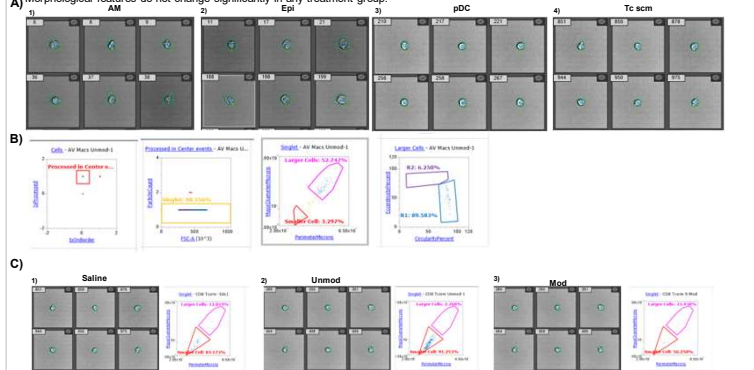


Figure 7. Confirming sort results using Image Enhanced Flow Cytometry (IEFC) on the Invitrogen™ Attune™ Cytipix

To verify the identity and confirm the morphology of the sorted cells, they were acquired and imaged using the Cytipix camera on the Attune cytometer. (A) Sample images of (1) AM, (2) Epi, (3) pDCs and (4) Tc scm cell subsets show that macrophages and Epithelial cells appear larger while pDCs and Tc scm appear smaller. High parameter imaging data analysis was performed. The resulting gating strategy (B) identifies processed, singlet events that could be divided into larger and smaller cells based on perimeter and major diameter and then further subtyped into round and eccentric cells. (C) Images and size analysis of Tc scm cells after sorting from (1) saline, (2) Unmod, or (3) mod mouse groups. Morphological features do not change significantly in any treatment group.



Conclusions

- 36 subpopulations from both immune and non-immune origin were identified using the 25 parameter immunophenotyping panel
- Immune changes due to immunomodulation could be monitored easily and reproducibly
- The target cells for the LNPs were predominantly lung endothelial cells
- Our data suggest that CD45+ cells were not targeted by the LNP-mRNA treatment, however their frequency and marker expression still changed to more inflammatory phenotypes
- Inflammatory immune changes were exclusively seen in the Unmod group and not in the Mod group suggesting that the LNP did not cause immune modulation, but the mRNA did
- Cells could be sorted from the lung with high sorting efficiency regardless of treatment type
- Image enhanced flow cytometry and AI based image analysis were used to confirm the identity of sorted cells. Image analysis confirmed that the Tc scm subset was composed entirely of small lymphocytes before and after immune modulation and was not contaminated by a Sca-1 expressing tissue derived larger cell subset

Acknowledgements

We would like to thank Daniel Rose for sorting help, Sammy Ellis for instrument maintenance, Brandon Neidner for Attune training, Manisha Chadwani for AI software training, The ThermoFisher CAI/ CST team for helpful discussions and feedback.

Trademarks/Licensing

© 2024 Thermo Fisher Scientific Inc. All rights reserved. For research Use Only. Not for use in diagnostic procedures. All trademarks are the property of Thermo Fisher Scientific and its subsidiaries unless otherwise specified. This information is not intended to encourage use of these products in any manner that might infringe the intellectual property rights of others. Mouse work performed by Virginia Aragon (ThermoFisher Scientific) in accordance with animal use and ethics policies. Lipid nanoparticles #VFS2201 provided by Virginia Aragon.